

Effectiveness of near-infrared light photodynamic therapy on oral cancer cells

*Jinhao Cui¹, Tomoharu Okamura², Chihoko Ikeda², Kazuya Tominaga² and Akio Tanaka³

¹Graduate School of Dentistry (Department of Pathology), ²Department of Oral Pathology, ³Department of Pathology, Osaka Dental University, 8-1Kuzuhahanazono-cho, Hirakata-shi, Osaka 573-1121, Japan

*Email: cui-j@cc.osaka-dent.ac.jp

Oral cancer is a common malignant cancer, which is difficult to treat with traditional methods. Photodynamic therapy is a new alternative that is gaining widespread attention. We investigated the therapeutic effectiveness against oral cancer cells, and the mechanism of action of near-infrared photodynamic therapy (NIR-PDT) combined with the photosensitizer Chlorin e6 (Ce6) and up-conversion nanoparticles NaYF₄:Yb/Er (UCNPs). After using the MTT (3-(4,5-dimethyl-2-yl)-2,5-diphenyltetrazolium bromide) assay to determine a suitable concentration combination, human squamous cell carcinoma cells (HSC-3s) were treated with NIR-PDT combined with Ce6 and UCNPs. We examined cell proliferation and death by MTT assay, cell membrane permeability by live or dead cell staining, apoptosis by the FITC-Annexin V/PI assay, intracellular singlet oxygen and reactive oxygen species (ROS). NIR-PDT with 0.5ng/ μ L Ce6 and 0.1ng/ μ L UCNPs inhibited the cell proliferation of HSC-3s ($p < 0.05$). NIR-PDT led to an increase in intracellular singlet oxygen and ROS ($p < 0.05$), and changes in mitochondrial membrane potential and apoptosis occurred ($p < 0.01$). At the same time, the permeability of the cell membrane increased over time ($p < 0.05$). These results suggest that this treatment can inhibit the proliferation of oral cancer cells and induce apoptosis. (J Osaka Dent Univ 2024; 58: 125-134)

Key words: Photodynamic therapy; Oral squamous cell carcinoma; Cell membrane permeability; Apoptosis

INTRODUCTION

Oral cancer is a common head and neck cancer, with more than 300,000 cases worldwide each year.¹⁻³ The number of cases in Japan has increased every year between 2016 and 2019, accounting for 2.3% of all cancer patients in 2019.⁴ Because the covering epithelium of the oral mucosa is a stratified flattened epithelium, histopathologically more than 90% of oral cancers are squamous cell carcinomas (OSCCs).⁵⁻⁷ OSCC is similar to cancers of other organs in that heterogeneous tumor cells grow in an infiltrative pattern and tend to metastasize to regional or distant sites. For cancer, the usual treatment is surgery combined with chemotherapy and radiotherapy, and the five-year survival rate after treatment is less than 50% in the world. In addition, there are many side ef-

fects that impact the quality of life of the patient.^{6, 8}

Photodynamic therapy (PDT) is a new means of diagnosing and treating this disease. It kills cancer cells by generating reactive oxygen species (ROS) through the combination of light and a photosensitizer (PS), and causes a series of oxidative stress reactions.^{2, 9, 10} Light sources include visible light, near-infrared light (NIR), as well as other forms, and the PS includes endogenous cellular components and natural compounds. Since cancer tissues selectively absorb PS, the accumulation in normal tissue is reduced. It is possible to limit the damage to normal tissues to that of a self-healing burn produced by light exposure.^{8, 11} The three main types of cell damage from PS are apoptosis, necrosis and autophagy. This depends on the type and intracellular localization of the PS, as well as the intensity of the light exposure.¹²⁻¹⁴ Apoptosis is programmed

cell death and the main form of cell death after PDT. It is divided into early and late apoptosis. Normally, early apoptotic cells maintain membrane integrity, while late apoptotic cells exhibit characteristics similar to necrosis. Necrosis differs from apoptosis in that it is a passive, unexpected death. It is often accompanied by destruction of cell membranes and an inflammatory response.¹⁵⁻¹⁷

The light source used in this study was NIR at 980 nm. NIR directed into the bio-optical window has high tissue penetration and causes relatively little light damage to the biological tissues. NaYF₄:Yb/Er is a typical up-conversion nanoparticle that can convert long-wave radiation to short-wave radiation.¹⁸ Ce6, a second generation photosensitizer (PS), is used in many diseases other than cancer.¹⁹ The combined use of the two can produce better results under NIR conditions. The combination is synthesized as a series of complex chemical reactions, including precursor formation, several rounds of centrifugation, and pyrolysis.²⁰ We investigated the optimal combination for the concentrations of these two substances for direct use without chemical bonding, and the appropriate light intensity to observe the therapeutic effects.

MATERIALS AND METHODS

Cell culture

The HSC-3 cell line was provided by the Second Department of Oral and Maxillofacial Surgery, Osaka Dental University. The cells were cultivated in high glucose Dulbecco's Modified Eagle Medium (DMEM; Nacalai Tesque, Kyoto, Japan) supplemented with 10% fetal bovine serum (FBS; Biowest, Nuaille, France), 5% HEPES buffer solution (Dojindo Laboratories, Kumamoto, Japan) and 1% P-S-A (Nacalai Tesque) at 37°C and 5% carbon dioxide.

Preparation of photosensitizer and up-conversion particles

One stock solution was prepared by adding 2 mL of FBS(-) DMEM to 1,000 mg Chlorin e6 (Ce6; Fujifilm Wako Pure Chemical, Osaka, Japan). The medium with Ce6 was adjusted to each concentration

with FBS(-) DMEM. An additional stock solution was prepared by adding 1 mL of distilled water to NaYF₄:Yb/Er (UCNPs; Filgem, Nagoya, Japan). The UCNP medium was adjusted to each concentration with phosphate buffered saline (PBS; Fujifilm Wako Pure Chemical), and stored at 4°C until use.

Measurement of Ce6 fluorescence

To determine the accumulation of photosensitizer in the cells, Ce6 (0.5 ng/ μ L) and UCNPs (0.1 ng/ μ L) were added to each well after 24 h of incubation. The fluorescence intensity was observed after 1, 2, 3 and 4 hours using a microplate reader (Molecular Devices, San Jose, CA, USA) at Ex 405 nm and Em 650 nm.²¹

MTT Assay

In order to determine the optimal concentration of the combinations of Ce6 and the UCNPs, and the effect of different light intensities on cells, we did cell proliferation experiments using the MTT Cell Proliferation Assay Kit (Cayman Chemical, Ann Arbor, USA). The concentration of Ce6 was first adjusted to 0, 0.1, 0.5, 1.0, 10 and 100 ng/ μ L, and that of the UCNPs was adjusted to 0, 0.1, 1.0, 10 and 100 ng/ μ L. Cells at 2.5×10^4 cells/mL were seeded on 96-well microplates and incubated for 24 hours. After washing with PBS, the cells were placed in an incubator (37°C, 5% CO₂) with the various concentrations of Ce6 and the UCNPs for three hours. They were then washed with PBS and the medium was replaced with fresh medium. Twenty-four hours later, 10 μ L of MTT reagent was added to each well. The solutions were mixed gently for one minute in an orbital shaker and incubated at 37°C in 5% CO₂. After four hours, 100 μ L of crystal dissolving solution was added to each well, and the cells were incubated for 8 hours in 37°C. Similarly, to determine the optimal treatment conditions, the cells were treated with different intensities of light as well as different concentrations of photosensitizer at the same light intensity after adding the same concentration of photosensitizer. Cell proliferation was assayed as described above. The absorbance of each sample was measured at

570 nm using a microplate reader.

Photodynamic therapy

The human squamous cell carcinoma cells-3 (HSC-3s) were incubated with Ce6 and the UCNPs for three hours. Cells were then exposed to a light dose of 5 J/s ($0.5W \times 10s$) from a semiconductor laser with a wavelength of 980nm (Wuhan Pioon Technology, Wuhan, China).

Measurement of intracellular singlet oxygen

After NIR-PDT, the cells were washed twice with Hanks' Balanced Salt Solution (HBSS), and a working solution of 100 μ L Si-DMA (Si-DMA for Mitochondrial Singlet Oxygen Imaging; Dojindo Laboratories) was added to each well. The cells were then incubated for 45 min at 37°C. Fluorescence intensity was measured and analyzed by confocal laser scanning microscopy (LSM700; Carl Zeiss, Oberkochen, Germany) and Image J Software (National Institutes of Health, Bethesda, Maryland, USA) at Ex 630-680 nm and Em 660-680 nm.

Measurement of intracellular reactive oxygen species (ROS)

After NIR-PDT, the cells were washed twice with HBSS, and a working solution of 100 μ L ROS (ROS Assay Kit-Highly Sensitive DCFH-DA; Dojindo Laboratories) was added to each well. The cells were then incubated for 30 min at 37°C. Fluorescence intensity was analyzed with the microplate reader at Ex 490-520 nm and Em 510-540 nm.

Detection of change in mitochondrial membrane potential

The mitochondrial membrane potential was examined with a JC-1 MitoMP Detection Kit (Dojindo Laboratories). Cells were seeded at 2.5×10^4 cells/mL on a 96-well plate and incubated for 24 h. After NIR-PDT, the medium was removed and the cells were incubated with fresh culture medium containing 4 μ mol/L JC-1 working solution at 37°C in the dark. Forty minutes later, the cells were washed twice with HBSS and an imaging buffer solution was added to each well. The fluorescence change

was analyzed using a confocal laser scanning microscope with the settings for green at Ex 488 nm and Em 500-550 nm, and red at Ex 561 nm and Em 560-610 nm.

Changes in cell membrane damage

A Live/Dead Cell Staining Kit II (PromoCell, Heidelberg, Germany) was used to measure the changes in membrane status. This kit provides two-color fluorescent staining of Calcein-AM (live cells) and EthD-III (dead cells).²² HSC-3 cells were seeded on a 96-well plate and incubated for 24 h. To make the working solution, 2.5 μ L of 4 mM Calcein-AM and 10 μ L of 2 mM EthD-III were added to 5 mL of PBS. After the NIR-PDT, the cells were washed twice with PBS and incubated in 100 μ L PBS and 100 μ L working solution at room temperature for 40 min. The fluorescence intensity was measured immediately after treatment and at 30 min, 1 h and 2 h, with a microplate reader (Calcein-AM: Ex 495nm, Em 515nm; EthD-III: Ex 530nm, Em 635nm).

Apoptosis assay

In order to detect cell apoptosis, an Annexin V-FITC apoptosis kit (Nacalai Tesque) was used according to the manufacturer's instructions. The staining solution was adjusted by adding 5 μ L of FITC-Annexin V and 5 μ L of PI solution. After 1 h of treatment, data acquisition and analysis were carried out using confocal laser scanning microscopy and flow cytometry (FACSverse; BD Biosciences, San Jose, CA, USA).

Statistical analysis

Relationships between the two groups were analyzed using Student's *t*-test. All analyses were carried out using Excel software (ver. 16.32), with all experiments repeated three times. A *p* value less than 0.05 was considered statistically significant.

RESULTS

Photosensitizer Ce 6 accumulation in HSC-3 cells

To determine the optimal time to implement pho-

totherapy, we examined the accumulation of photosensitizer in the cells. The fluorescence values began to increase 1 hr after the addition of the photosensitizer and reached the maximum at 3 hrs, after which they tended to decrease (Fig. 1). Therefore,

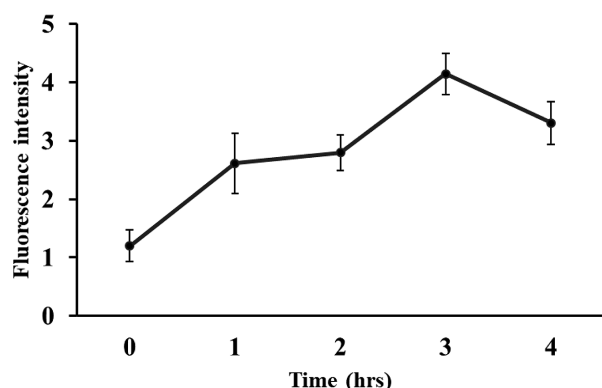


Fig. 1 Fluorescence intensity of Ce6 in HSC-3 cells at different incubation times.

a 3-hour incubation time was chosen for the following experiments.

NIR-PDT inhibits the proliferation of HSC-3 cells

The effect of PDT on cell proliferation was examined by MTT assay. Concentrations of Ce6 at 0.1 and 0.5 ng/ μ L, and of UCNPs at 0.1 ng/ μ L had no significant effect on the cells (Figs. 2A and B). After combining the two and treating cells with NIR, the cell survival rate was 64% and 57% (Fig. 2C). At the same concentration of Ce6 (0.5 ng/ μ L) and the UCNPs (0.1 ng/ μ L), but with different intensities of NIR, the survival rate did not change much between 0.5 and 1.5 Watts, but then started to decrease again after 2Watts (Fig. 2D). *In vitro*, NIR-PDT inhibited proliferation with the combination of 0.5 ng/ μ L Ce6 + 0.1 ng/ μ L UCNPs at 0.5Watts for 10s.

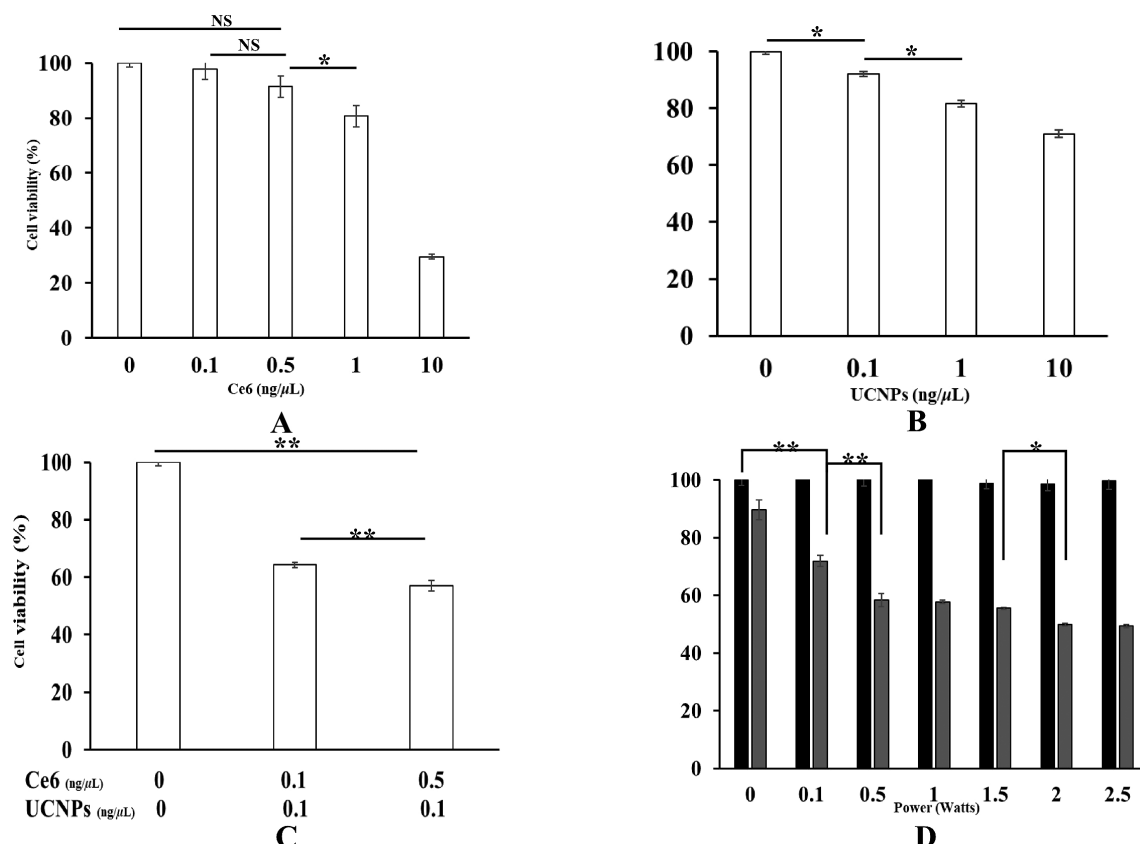


Fig. 2 Effect of Ce6, UCNPs and NIR-PDT on cell proliferation (A) for different concentrations of Ce6 without NIR-PDT, (B) for different concentrations of UCNPs without NIR-PDT, (C) with Ce6 and UCNPs for different combinations of concentrations with NIR-PDT (5J), and (D) with varying light intensity only or with Ce6 at 0.5 ng/ μ L and UCNPs at 0.1 ng/ μ L. (■ Ce6-UCNPs-, ■ Ce6-UCNPs+, * p < 0.05, ** p < 0.01, NS: Not significant).

Increase in intracellular singlet oxygen

The generation of singlet oxygen was examined in NIR-PDT-treated HSC-3 cells. As shown in Fig. 3 A, the average fluorescence intensity increased after NIR-PDT with Ce6 and UCNPs compared with

the control, Ce6-UCNPs, or the laser alone group. The fluorescence emission of only NIR-PDT-treated cells showed red, indicating an increase in intracellular singlet oxygen (Fig. 3 B).

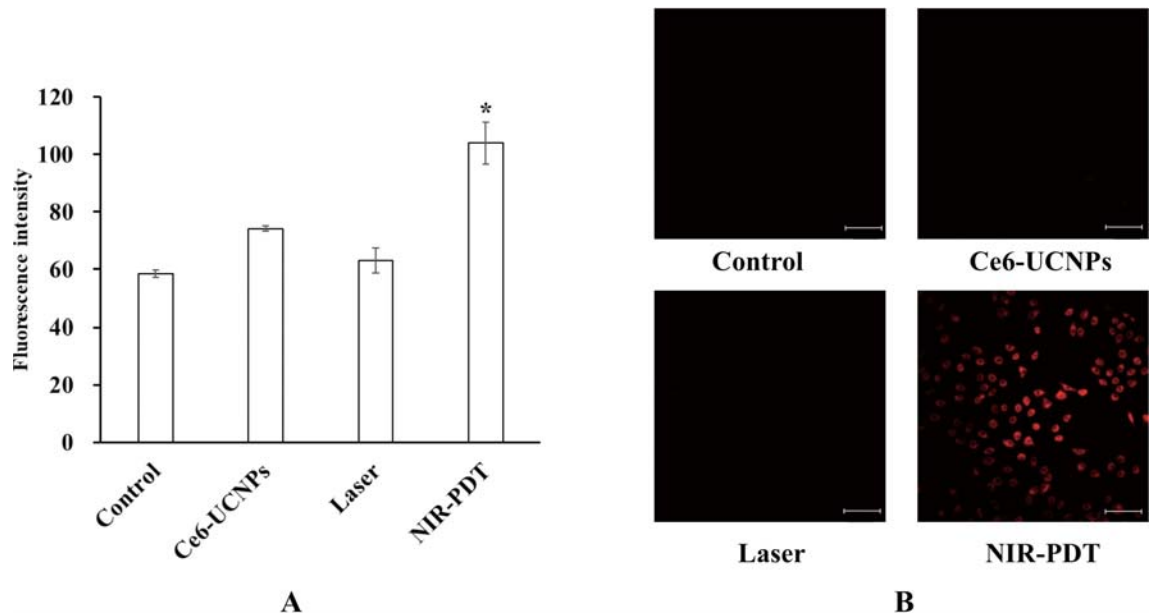


Fig. 3 Effect of various treatments on HSC-3 cells. The data was analyzed using (A) Image J Software and (B) confocal laser scanning microscopy (Control: No treatment; Ce6-UCNPs: Ce6-UCNPs only; Laser: NIR only; NIR-PDT: NIR-PDT+Ce6-UCNPs, Bar: 100 μ m, * p <0.05).

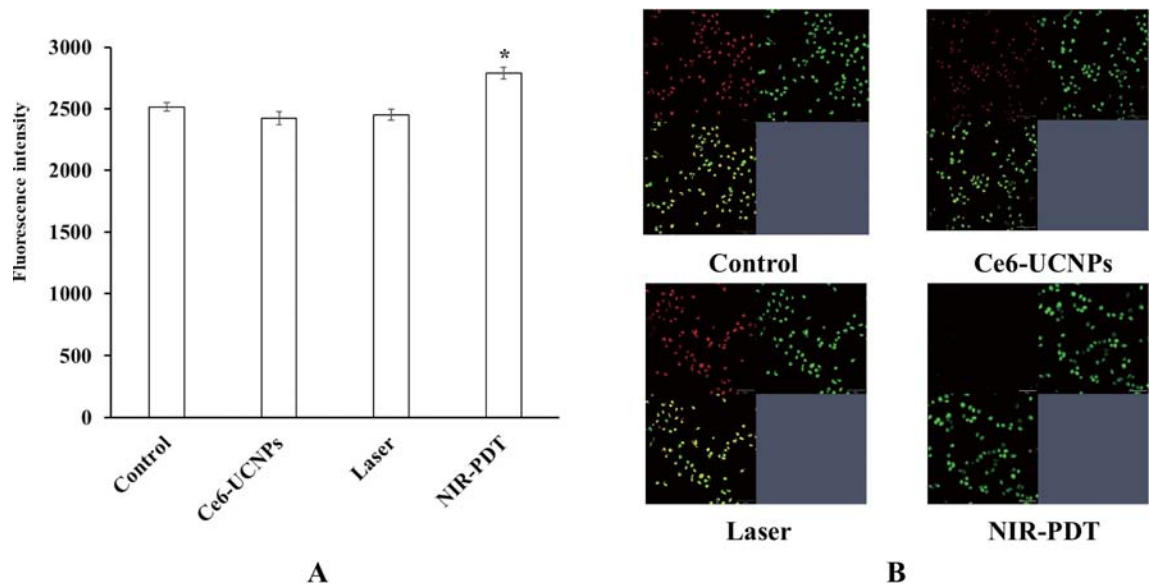


Fig. 4 Effect of various treatments on mitochondrial membrane potential changes in the HSC-3 cells. (A) This shows the fluorescence intensity of HSC-3 cells stained by DCFH-DA dye after treatment with laser irradiation. (B) The cells were stained with JC-1 dye and analyzed using confocal laser scanning microscopy (Control: No treatment; Ce6-UCNPs: Ce6-UCNPs only; Laser: NIR only; NIR-PDT: NIR-PDT+Ce6-UCNPs, Bar: 100 μ m, * p <0.05).

ROS production and mitochondrial membrane potential change

Although there was an increase in the amount of reactive oxygen species compared to the controls, it was less pronounced (Fig. 4 A). Mitochondria are

the main site of reactive oxygen species production,⁶ and we also observed changes in mitochondrial membrane potential. The experimental (NIR-PDT) group with lower membrane potential had stronger green fluorescence, while the control group had stronger red fluorescence (Fig. 4 B).

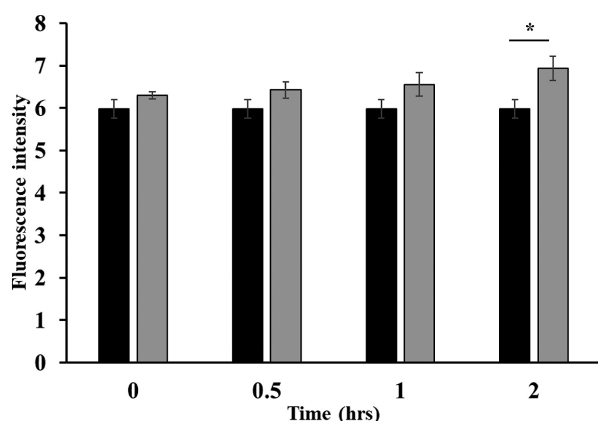


Fig. 5 Changes in cell membrane damage at different times after NIR-PDT (■ Control, ■ NIR-PDT, * $p < 0.05$).

Increase in cell membrane damage

The intensity of the green fluorescence, which represents living cells, was reduced under near-infrared light. The intensity of red fluorescence, which reflects the degree of cell membrane damage, did not change significantly immediately after treatment, but gradually increased over time (Fig. 5). This indicates that the change in cell membrane permeability is related to the time after treatment.

NIR-PDT induced apoptosis

Apoptosis was analyzed by Annexin V/PI staining. Compared with the control group, apoptotic cells in-

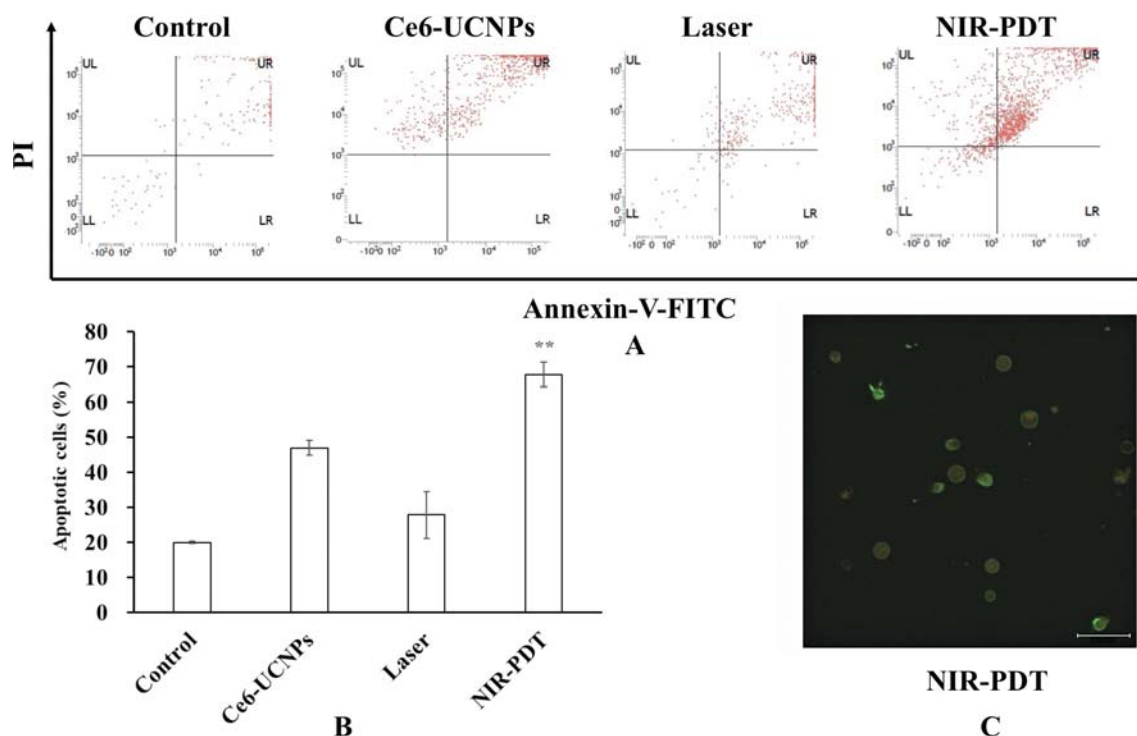


Fig. 6 Apoptosis analysis of HSC-3 cells by the FITC-Annexin V/PI Staining Assay. (A and B) (LL: Normal cells; LR: Annexin V-positive and PI-negative early apoptosis cells; UR: Annexin V-positive and PI-positive late apoptosis cells; UL: Necrotic cells). (C) Green indicates early apoptosis cells, while green and red indicate late apoptosis cells (Control: No treatment; Ce6-UCNPs: Ce6-UCNPs only; Laser: NIR only; NIR-PDT: NIR-PDT + Ce6-UCNPs, Bar: 100 μ m, ** $p < 0.01$).

creased after treatment and were positive for both Annexin V and PI (Figs. 6 A and B). Apoptotic cells showing both green and red fluorescence were also observed by fluorescence microscopy (Fig. 6 C).

DISCUSSION

In treating a disease, in addition to considering a successful cure, attention should also be paid to the patient's quality of life after treatment. Oral cancer that occurs in the maxillofacial region affects not only the survival of the patient, but also is associated with future problems with eating, speech and aesthetics. The initial symptoms of oral cancer are not obvious. It is often only detected during the late stages. Treatment requires surgery combined with radiotherapy and chemotherapy, a long-term intervention that negatively affects the patient's quality of life.²³ A study by Barrios Rocío *et al.* showed that patients treated for oropharyngeal cancer had a significantly poorer quality of life than the general population.²⁴

As an alternative treatment, photodynamic therapy aims to achieve targeted therapeutic effects, thereby reducing postoperative adverse situations or even eliminating the need for chemo-radiotherapy.¹⁷ The specific vascular microenvironment of tumors, such as defective cellular linings, loosely connected epithelial cells, and weak lymphatic drainage, can result in the preferential aggregation of treatment drugs in tumors when administered systemically. The same is true for photosensitizers as agents, which are more destructive to tumor tissue when exposed to light.²⁵⁻²⁷ In the *in vitro* tests of this study, although the photosensitizer and upconversion nanoparticles were not chemically bonded, they had an effect on the proliferation of the HSC-3 cells. There was a significant difference in cell viability between treatment without UCNPs and treatment with UCNPs at 0.1 ng/ μ L. Comparing the measured values, the values for UCNPs at 0 ng/ μ L, 0.1 ng/ μ L and 1.0 ng/ μ L were 0.38, 0.35 and 0.31, respectively. Therefore, since 0.1 ng/ μ L was the lowest effective concentration of UCNPs investigated, was adopted this concentration in our study. We used 0.5ng/ μ L of Ce6 and 0.1ng/ μ L of UCNPs.

The NIR-PDT of HSC-s-implanted carcinoma-bearing nude mice after injection of a 5:1 ratio of Ce6: UCNPs resulted in partial disappearance of cancer cells (data not shown). In the PDT response, both electron shifters (Type I) and/or energy shifters (Type II) usually occurred.²⁸⁻³⁰ The experimental results showed that the treatment led to the production of Type II reactive oxygen species and single linear oxygen species. On the whole, the elevation of ROS was not significant. With visible light experiments, especially with plasma membrane-targeted photosensitizers, ROS is generally the main product and the main cause of plasma membrane damage. In contrast, it is not the main cause in near-infrared (NIR) photo-immunotherapy.^{22, 31} Although this experiment did not use an immune-targeted photosensitizer, the same NIR may have produced results that are intermediate between the above two types. At the same time, there were some changes in the mitochondrial membrane potential. It may indicate that apoptosis occurs in association with the mitochondrial pathway.^{32, 33}

Photodynamic therapy can cause cell death through a variety of pathways, among which apoptosis is the most common.³⁴ It is a complex process, regulated by various genes, and can occur before the first mitosis (early apoptosis) or as the final step of mitotic catastrophe (late apoptosis). Cell shrinkage, apoptotic body formation, and DNA fragmentation are typical features.^{35, 36} In this experiment, apoptosis was detected by flow cytometry and fluorescence microscopy using fluorescein isothiocyanate (FITC)-conjugated Annexin V (Annexin V-FITC) and propidium iodide (PI). Annexin-V is a calcium-dependent phospholipid-binding protein, and when apoptosis occurs, phosphatidylserine, which is located on the inner side of the cell, is exposed on the surface of the cell membrane, where it is recognized by Annexin-V and produces green fluorescence.³⁷ After treatment, the results of flow cytometry revealed Annexin V/PI-double-positive (Annexin V-FITC+/PI+) late apoptotic cells, while the results of microscopy showed the presence of both early and late apoptotic cells. PI dye cannot pass

through the cell membrane, and can only enter when the cell membrane is damaged and the permeability changes, eventually showing red fluorescence.^{38, 39}

In the experimental results we found a slightly higher positivity rate in the individual control groups as well. This is because when using flow cytometry to detect apoptosis, the cells must be free. The use of trypsin stripping and PBS rinsing of adherent cells may cause damage to the cell membrane, resulting in false positives. Moreover, different cancer cell lines have different membrane sensitivities.⁴⁰⁻⁴² However, overall, the positive rate of the experimental group was still higher than that of the controls. Generally, apoptotic cells maintain membrane integrity, and membrane damage occurs during necrosis. However, recent studies have shown that secondary necrotic apoptotic cells also undergo cell membrane damage. This phenomenon occurs when apoptotic cells are not cleared by scavenger cells in time.⁴³ This may be one reason for the PI positive phenomenon in this experiment. However, whether the cells in this experiment were in secondary necrosis after apoptosis or primary necrosis cannot be determined at present. Because both are Annexin V-FITC + /PI +, the difference between them cannot be determined using only the detection method of this experiment, and these fluorescent stains may interfere with the apoptosis mechanism.

In Brauchle's study, specific death mechanisms could be distinguished using Raman microspectroscopy to examine the state of individual cells.³⁶ The results of live/dead cell staining have also shown that the cell membrane permeability increases with time. In living cells the conversion of calcine-AM to the strongly fluorescent calcineurin produces an intense and uniform green fluorescence due to the action of the enzyme endostatin. Although an intact plasma membrane of living cells blocks EthD-III, dead cells are usually characterized by damaged cell membranes. EthD-III enters dead cells and produces bright red fluorescence upon binding to nucleic acids.²²

Although the disappearance of a part of the tu-

mor tissue as well as apoptosis can be observed *in vivo*, scattered cancerous tissue can still be seen in the other parts of tissue (data not shown). This may be related to the duration of light exposure versus the dose of the drug. When Ce6 and UCNP are not chemically bonded, they have a certain level of therapeutic effect and can be used as a simple basic treatment. There is a close connection between changes in the cell membrane and cell death, which is something that needs to be further considered and investigated under the conditions of this experiment.

Acknowledgments

This work was supported by Osaka Dental University Research Funds [23-02]. The authors have no conflicts of interest to disclose for this study.

REFERENCES

1. Balian GMFC, Luiz MT, Filippo LDD, Chorilli M. Mucoadhesive liquid crystal precursor system for photodynamic therapy of oral cancer mediated by methylene blue. *Photodiagn Photodyn Ther* 2023; **44**: 103739.
2. Longo JPF, Lozzi SP, Simioni AR, Morais PC, Tedesco AC, Azevedo RB. Photodynamic therapy with aluminum-chlorophthalocyanine induces necrosis and vascular damage in mice tongue tumors. *J Photochem Photobiol B Biol* 2009; **94**: 143-146.
3. Kawakita D, Oze I, Iwasaki S, Matsuda T, Matsuo K, Ito H. Trends in the incidence of head and neck cancer by subsite between 1993 and 2015 in Japan. *Cancer Med* 2022; **11**: 1553-1560.
4. Cancer Statistics. Cancer Information Service, National Cancer Center, Japan (National Cancer Registry, Ministry of Health, Labour and Welfare). [https://ganjoho.jp/reg_stat/statistics/data/dl/excel/cancer_incidenceNCR\(2016-2019\).xls](https://ganjoho.jp/reg_stat/statistics/data/dl/excel/cancer_incidenceNCR(2016-2019).xls): accessed on July 30, 2023.
5. Rivera C. Essentials of oral cancer. *Int J Clin Exp Pathol* 2015; **8**: 11884-11894.
6. Ahn MY, Yoon HE, Kwon SM, Lee J, Min K, Kim YC, Ahn SG, Yoon JH. Synthesized pheophorbide a-mediated photodynamic therapy induced apoptosis and autophagy in human oral squamous carcinoma cells. *J Oral Pathol Med* 2013; **42**: 17-25.
7. Takagi M, Toyosawa S, Takata T, Atlas of Oral Pathology. 3rd ed. Tokyo: Bunkodo, 2018: 235-239.
8. Yang TH, Chen CT, Wang CP, Lou PJ. Photodynamic therapy suppresses the migration and invasion of head and neck cancer cells in vitro. *Oral Oncol* 2007; **43**: 358-365.
9. Inoue K, Fukuhara H, Kurabayashi A, Furihata M, Tsuda M, Nagakawa K, Fujita H, Utsumi K, Shuin T. Photodynamic therapy involves an angiogenic mechanism and is enhanced by ferrochelatase inhibitor in urothelial carcinoma. *Cancer Sci* 2013; **104**: 765-772.
10. Selbo PK, Hogset A, Prasmickaite L, Berg K. Photochemical internalization: a novel drug delivery system. *Tumor Biol* 2002; **23**: 103-112.

11. Ivanova-Radkevich VI. Biochemical basis of selective accumulation and targeted delivery of photosensitizers to tumor tissues. *Biochemistry Moscow* 2022; **87**: 1226-1242.
12. Anigo EC, George BP, Abrahamse H. Molecular effectors of photodynamic therapy-mediated resistance to cancer cells. *Int J Mol Sci* 2021; **22**: 13182.
13. Olsen CE, Weyergang A, Edwards VT, Berg K, Brech A, Weisheit S, Høgset A, Selbo PK. Development of resistance to photodynamic therapy (pdt) in human breast cancer cells is photosensitizer-dependent: possible mechanisms and approaches for overcoming pdt-resistance. *Biochem Pharmacol* 2017; **144**: 63-77.
14. Agostinis P, Buytaert E, Breysens H, Hendrickx N. Regulatory pathways in photodynamic therapy induced apoptosis. *Photochem Photobiol Sci* 2004; **3**: 721-729.
15. Patel VA, Longacre A, Hsiao K, Fan H, Meng F, Mitchell JE, Rauch J, Ucker DS, Levine JS. Apoptotic cells, at all stages of the death process, trigger characteristic signaling events that are divergent from and dominant over those triggered by necrotic cells. *J Biol Chem* 2006; **281**: 4663-4670.
16. Fink SL, Cookson BT. Apoptosis, pyroptosis, and necrosis: mechanistic description of dead and dying eukaryotic cells. *Infect Immun* 2005; **73**: 1907-1916.
17. Dube A, Sharma S, Gupta PK. Tumor regression induced by photodynamic treatment with chlorin p6 in hamster cheek pouch model of oral carcinogenesis: dependence of mode of tumor cell death on the applied drug dose. *Oral Oncol* 2011; **47**: 467-471.
18. Mahata MK, De R, Lee KT. Near-infrared-triggered upconverting nanoparticles for biomedicine applications. *Biomedicine* 2021; **9**: 756.
19. Ryu AR, Lee MY. Chlorin e6-mediated photodynamic therapy promotes collagen production and suppresses MMPs expression via modulating AP-1 signaling in P. acnes-stimulated HaCaT cells. *Photodiagn Photodyn Ther* 2017; **20**: 71-77.
20. Chen G, Qiu H, Prasad PN, Chen X. Upconversion nanoparticles: design, nanochemistry, and applications in theranostics. *Chem Rev* 2014; **114**: 5161-5214.
21. Kulichenko A, Farrakhova DS, Yakovlev DV, Maklygina YS, Shiryayev AA, Loschenov VB. Fluorescence diagnostics and photodynamic therapy of squamous cell carcinoma of the lateral surface of the tongue using the photosensitizer chlorin e6 by spectroscopic video fluorescence methods. *J Phys: Conf Ser* 2021; **2058**: 012021.
22. Nakajima K, Takakura H, Shimizu Y, Ogawa M. Changes in plasma membrane damage inducing cell death after treatment with near-infrared photoimmunotherapy. *Cancer Sci* 2018; **109**: 2889-2896.
23. Meera M, Thiruneelakandan S, Thangavelu A, Varsha KP. Quality of health assessment in oral cancer patients postoperatively—a retrospective study. *Ann Oral Maxillofac Surg* 2022; **5**: 100202.
24. Barrios R, Bravo M, Gil-Montoya JA, Martínez-Lara I, García-Medina B, Tsakos G. Oral and general health-related quality of life in patients treated for oral cancer compared to control group. *Health Qual Life Outcomes* 2015; **13**: 9.
25. Shirasu N, Yamada H, Shibaguchi H, Kuroki M, Kuroki M. Potent and specific antitumor effect of CEA-targeted photoimmunotherapy. *Int J Cancer* 2014; **135**: 2697-2710.
26. Kobayashi H, Watanabe R, Choyke PL. Improving conventional enhanced permeability and retention (EPR) effects; what is the appropriate target? *Theranostics* 2013; **4**: 81-89.
27. Fang J, Nakamura H, Maeda H. The EPR effect: unique features of tumor blood vessels for drug delivery, factors involved, and limitations and augmentation of the effect. *Adv Drug Deliv Rev* 2011; **63**: 136-151.
28. Wang Y, Li Y, Zhang Z, Wang L, Wang D, Tang BZ. Triple-jump photodynamic theranostics: MnO₂ combined upconversion nanoplateforms involving a type-I photosensitizer with aggregation-induced emission characteristics for potent cancer treatment. *Adv Mater* 2021; **33**: 2103748.
29. Baptista MS, Cadet J, Mascio PD, Ghogare AA, Greer A, Hamblin MR, Lorente C, Nunez SC, Ribeiro MS, Thomas AH, Vignoni M, Yoshimura TM. Type I and type II photosensitized oxidation reactions: guidelines and mechanistic pathways. *Photochem Photobiol* 2017; **93**: 912-919.
30. Zhuang Z, Dai J, Yu MLi J, Shen P, Hu R, Lou X, Zhao Z, Tang BZ. Type I photosensitizers based on phosphindole oxide for photodynamic therapy: apoptosis and autophagy induced by endoplasmic reticulum stress. *Chem. Sci* 2020; **11**: 3405-3417.
31. Mitsunaga M, Ogawa M, Kosaka N, Rosenblum LT, Choyke PL, Kobayashi H. Cancer cell-selective *in vivo* near infrared photoimmunotherapy targeting specific membrane molecules. *Nat Med* 2011; **17**: 1685-1691.
32. Hwang HS, Shin H, Han J, Na K. Combination of photodynamic therapy (PDT) and anti-tumor immunity in cancer therapy. *J Pharm Investig* 2018; **48**: 143-151.
33. Lam M, Oleinick NL, Nieminen AL. Photodynamic therapy-induced apoptosis in epidermoid carcinoma cells reactive oxygen species and mitochondrial inner membrane permeabilization. *J Biol Chem* 2001; **276**: 47379-47386.
34. Mei Y, Xiao X, Fan L, Liu Q, Zheng M, Hamblin MR, Ni B, Yin R. In vitro photodynamic therapy of endothelial cells using hematoporphyrin monomethyl ether (hemoporphin): relevance to treatment of port wine stains. *Photodiagn. Photodyn. Ther* 2019; **27**: 268-275.
35. Alphonse G, Maalouf M, Montagne PB, Ardail D, Beuve M, Rousson R, Scholz GT, Fournier C, Lafrasse CR. p53-independent early and late apoptosis is mediated by ceramide after exposure of tumor cells to photon or carbon ion irradiation. *BMC Cancer* 2013; **13**: 151.
36. Brauchle EE, Thude SS, Brucker SY, Layland KS. Cell death stages in single apoptotic and necrotic cells monitored by Raman microspectroscopy. *Sci Rep* 2014; **4**: 4698.
37. Vermes I, Haanen C, Nakken HS, Reutelingsperger C. A novel assay for apoptosis flow cytometric detection of phosphatidylserine expression on early apoptotic cells using fluorescein labelled Annexin V. *J Immunol Methods* 1995; **184**: 39-51.
38. Baransi K, Dubowski Y, Sabbah I. Synergetic effect between photocatalytic degradation and adsorption processes on the removal of phenolic compounds from olive mill wastewater. *Water Res* 2012; **46**: 789-798.
39. Demchenko AP. Beyond annexin V: fluorescence response of cellular membranes to apoptosis. *Cytotechnology* 2013; **65**: 157-172.
40. Bundscherer A, Malsy MLange R, Hofmann P, Metterlein T, Graf BM, Gruber M. Cell harvesting method influences results of apoptosis analysis by Annexin V staining. *Anticancer Res* 2013; **33**: 3201-3204.
41. Engeland M, Ramaekers FC, Schutte B, Reutelingsperger CP. A novel assay to measure loss of plasma membrane asymmetry during apoptosis of adherent cells in culture. Cy-

- tometry* 1996; **24**: 131-139.
42. Wlodkowic D, Telford W, Skommer J, Darzynkiewicz Z. Apoptosis and beyond: cytometry in studies of programmed cell death. *Meth Cell Biol* 2011; **103**: 55-98.
43. Zhang Y, Chen X, Gueydan C, Han J. Plasma membrane changes during programmed cell deaths. *Cell Res* 2018; **28**: 9-21.